

Radiation campaign:

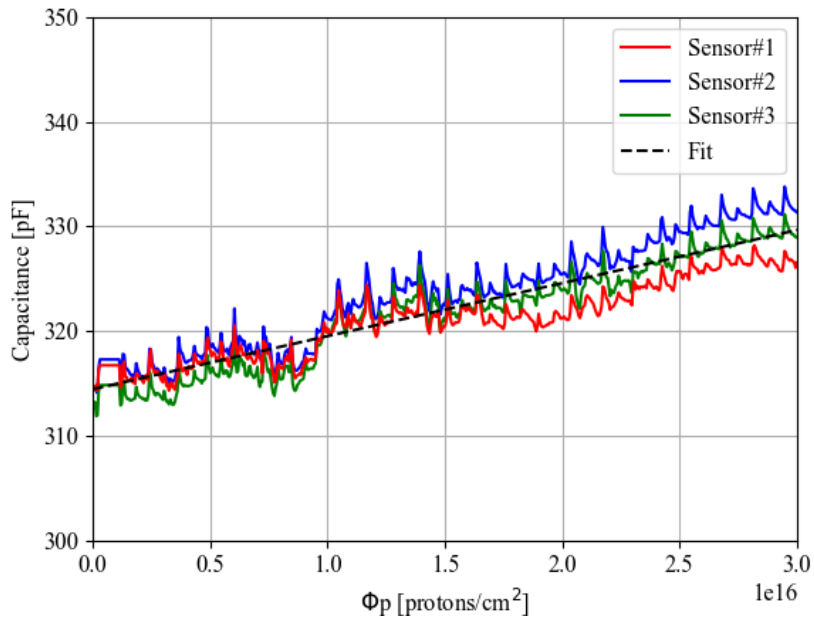


Fig. 1: Measurements were continuously taken during the irradiation of the samples.. The dependence of the sensor capacitance on the fluence can be described by a linear fit.

Magnetic test:

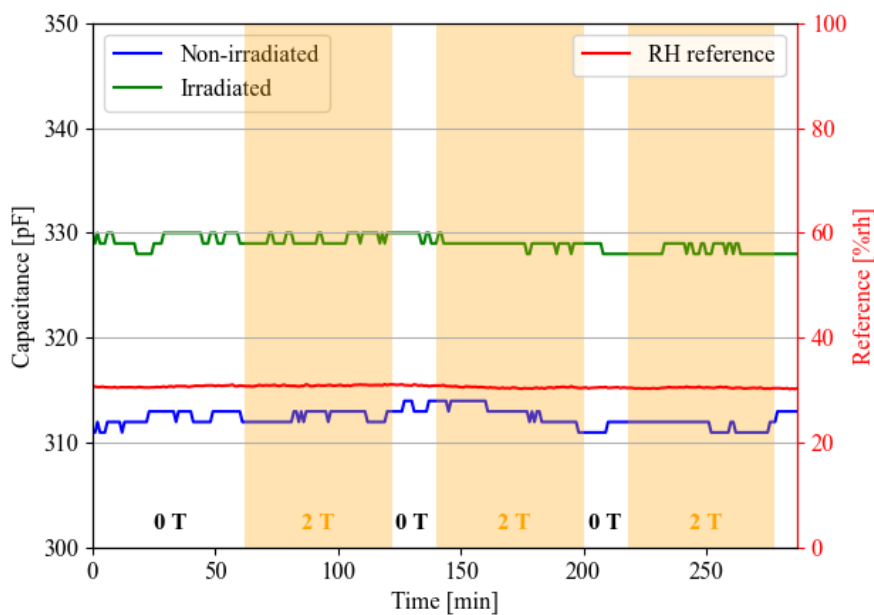
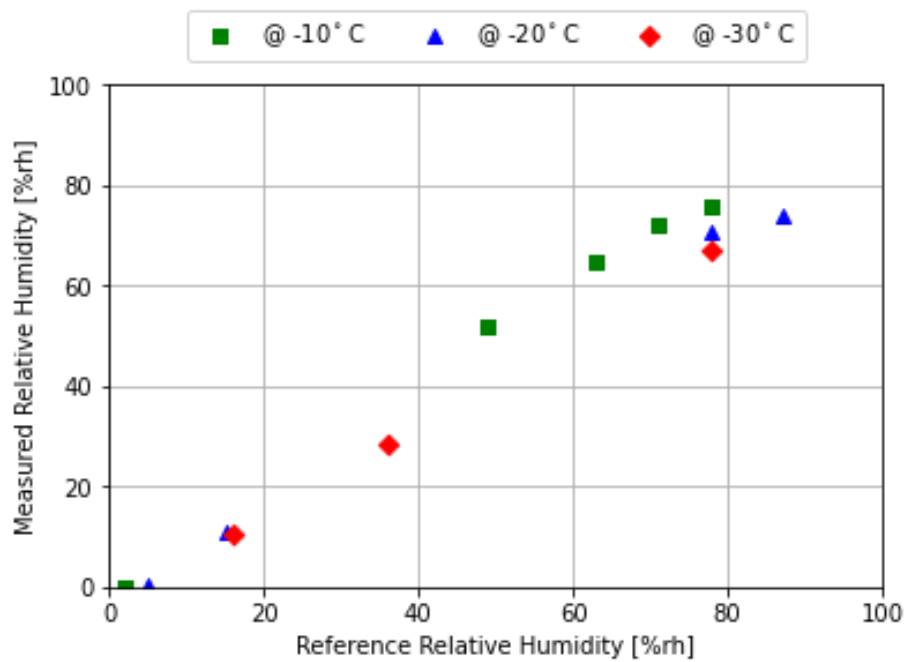
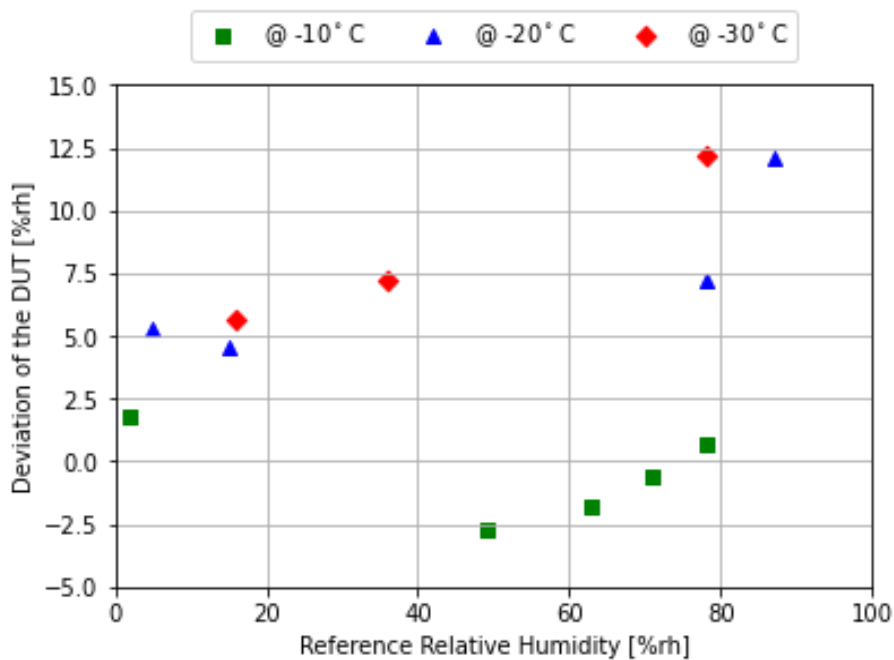


Fig. 2: Continuous monitoring when sensors tested in a 2 T magnetic field - the field strength of the ATLAS solenoid magnet and about 50 % of the field strength of the CMS solenoid.

Temperature dependence test:



(a)



(b)

Fig. 3: Average deviations of the devices under test with respect to the reference chilled mirror sensor (a) and the average difference between the reference chilled mirror and DUTs (b). The measurements were done at three different temperatures and various humidity levels.

One-channel readout unit:

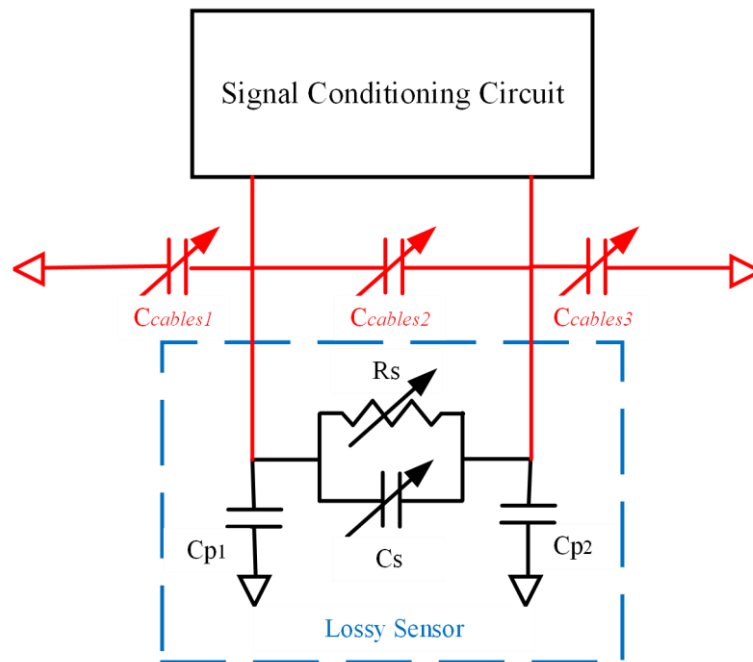


Fig. 4: *Equivalent electrical circuit for the leaky capacitive-based relative humidity sensor; where C_s represents the sensor capacitance, R_s is the internal sensor leakage resistance, and C_{p1} and C_{p2} are parasitic capacitance due to the sensor leads, while $C_{cables1}$, $C_{cables2}$ and $C_{cables3}$ are the parasitic capacitance of the cables.*

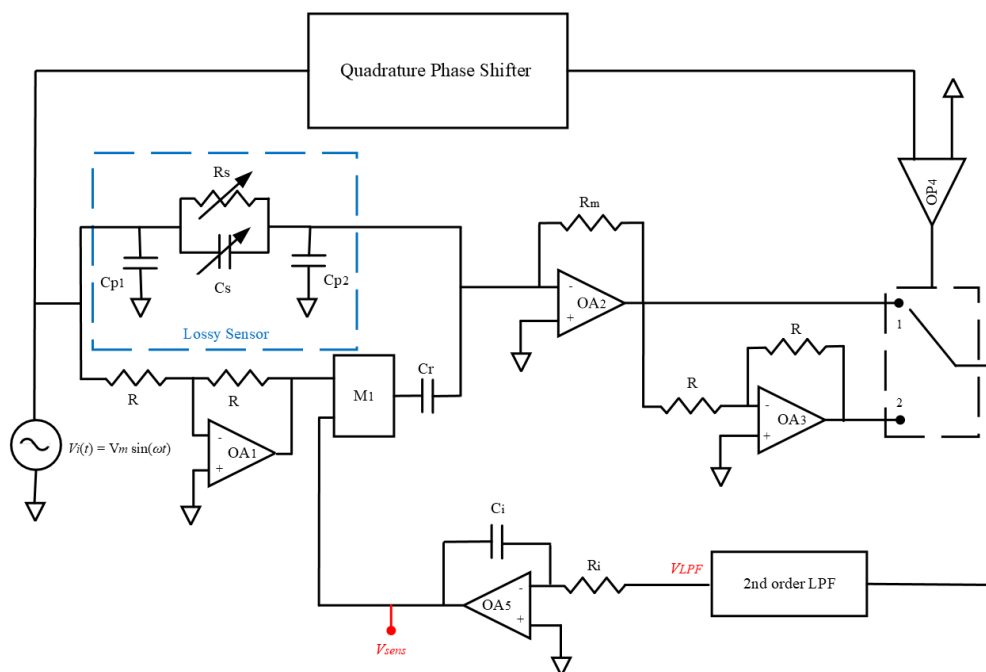


Fig. 5: *Schematic diagram of the signal conditioning circuit with a quadrature phase shifter; and auto-balancing bridge circuit. The quadrature phase shifter is used to separate the sensing capacitor from the bridge output signal.*

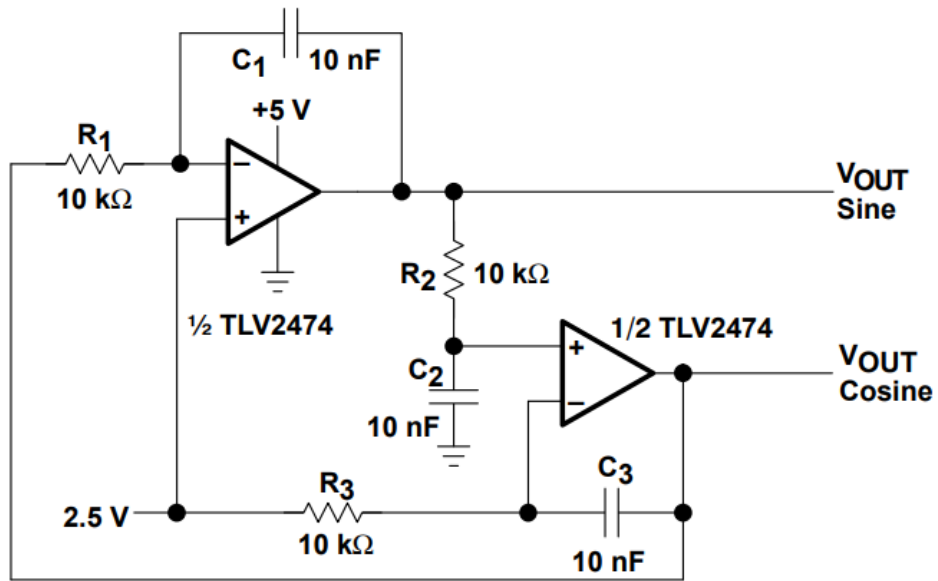


Fig. 6: On-board (quadrature) oscillator based on the TLV2474 chip and three RC networks for generating sine and cosine waves.